

Dynamics of Tearing Modes during Strong Electron Cyclotron Heating on the FTU Tokamak

E. Lazzaro,¹ A. Airoidi,¹ A. Bruschi,¹ P. Buratti,² S. Cirant,¹ R. Coelho,³ G. Granucci,¹ S. Nowak,¹ G. Ramponi,¹ A. Simonetto,¹ C. Sozzi,¹ O. Tudisco,² G. Bracco,² F. Crisanti,² F. Alladio,² B. Angelini,² M.L. Apicella,² G. Apruzzese,² E. Barbato,² L. Bertalot,² A. Bertocchi,² M. Borra,² G. Buceti,² A. Cardinali,² S. Cascino,² C. Centioli,² R. Cesario,² S. Ciattaglia,² V. Cocilovo,² R. De Angelis,² B. Esposito,² D. Frigione,² L. Gabellieri,² G. Gatti,² E. Giovannozzi,² M. Grolli,² F. Iannone,² H. Kroegler,² M. Leigheb,² G. Maddaluno,² M. Marinucci,² G. Mazzitelli,² P. Micozzi,² G. Monari,² P. Orsitto,² D. Pacella,² L. Panaccione,² M. Panella,² V. Pericoli,² L. Pieroni,² S. Podda,² G. Pucella,² G.B. Righetti,² F. Romanelli,² S. Sternini,² N. Tartoni,² A.A. Tuccillo,² V. Vitale,² G. Vlad,² V. Zanza,² M. Zerbini,² and F. Zonca²

¹*I.F.P.CNR, Assoc. EURATOM-ENEA-CNR, Via Cozzi 53, 20125 Milan, Italy*

²*C.R.E. ENEA, Assoc. EURATOM-ENEA-CNR, E. Fermi 45, Frascati, Italy*

³*Assoc. Euratom-IST, C.F.N. 1049-001, Lisboa, Portugal*

(Received 30 July 1999)

The localized electron cyclotron resonance heating power that can suppress sawteeth reconnection often drives $m = 2$ tearing modes in a tokamak operating at constant current. The dynamics of mode onset and coupled mode evolution is described in detail and compared with a nonlinear theoretical model that identifies the effects of mode coupling, finite inertia of the rotating islands, and wall braking.

PACS numbers: 52.35.Py

The observation of enhanced magnetohydrodynamic (MHD) fluctuations of the tearing type affecting the plasma energy transport in additionally heated tokamaks stimulates great interest in gathering experimental knowledge and understanding of the detailed mechanisms of these instabilities for finding a possible strategy for their active control in resistive and neoclassical regimes. In this Letter, we report the experimental evidence on the FTU tokamak and interpretation of two significant types of response of low order resistive MHD perturbations to the effects of temperature profile changes induced by localized heating. In one case the sawteeth instability is suppressed and an isolated $m = 2$ rotating tearing mode is driven; in another case $m = 1$ and $m = 2$ tearing modes are driven. We identify for the first time the detailed mechanism governing the rotation of toroidally coupled and uncoupled magnetic islands, associated to finite inertia and wall braking.

High power electron cyclotron resonance heating (ECRH) is used for controlling the MHD activity by fine adjustments of the position of the rf power absorbing layer [1,2]. The fundamental resonance scheme at 140 GHz was used. A power $P^{EC} \approx 800$ kW was injected in plasmas with major radius $R_0 = 0.97$ m, minor radius $a = 0.27$ m, toroidal magnetic field $B = (4-6)$ T, low plasma current ($I_p \approx 350$ kA) and high values of the safety factor $q(a) (\approx 6)$. At these $q(a)$ values, sawtooth relaxations are small or absent, while MHD oscillations with poloidal number $m = 2$ are observed in many cases. As a consequence of a moderate reshaping of the current density profile and of a substantial increase of the plasma pressure induced by ECRH near $q = 1$, MHD oscillations near $q = 2$ are strongly amplified (Fig. 1). The oscillations are detected by a fast electron cyclotron emission

(ECE) multichannel polychromator, by an array of detectors for soft-x-ray tomography, and by a set of Mirnov coils. Cross-correlation analysis shows that the poloidal and toroidal periodicity of these fluctuations is $m = 2$, $n = 1$ across most of the plasma section. In some cases, an $m = 1$, $n = 1$ component is detected in the central region. As shown in Fig. 2, the poloidal pattern of soft-x-ray emissivity has an even m periodicity that is confirmed by Mirnov coils signals to be $m = 2$. The phasing between the oscillations in the ECE and soft-x-ray diagnostics, placed at different toroidal angles, is consistent with an $n = 1$ toroidal order. The fast measurements of the electron temperature profile (Fig. 3), taken at different times during the island rotation, show a change in the slope around $r_{q=2}$ as the measurement happens to be alternatively on or near the "X" point ($t = 0.66035$ and $t = 0.6592$) and the "O" point during rotation. A

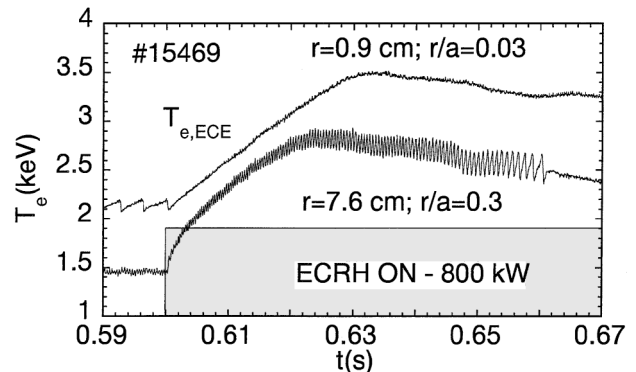


FIG. 1. T_e from two fast ECE channels (shot # 15469 with $B = 5.6$ T), tuned close to the plasma center (top) and to the position of maximum temperature oscillations (bottom).

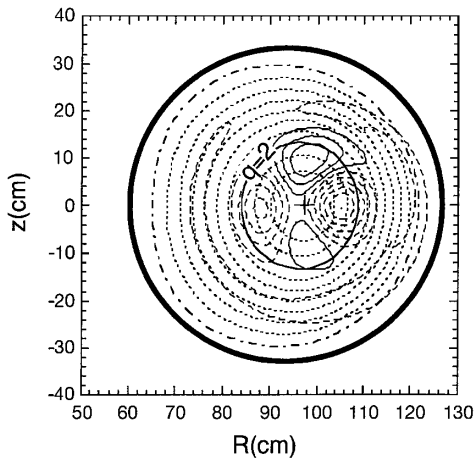


FIG. 2. Soft x-ray isoemission lines identifying the $m = 2$, $n = 1$ rotating magnetic island in shot # 15469. Dotted nested lines are equilibrium magnetic flux surfaces Ψ (from $\Psi = 0$ to $\Psi = 1$, step 0.1) The $q = 2$ surface is shown as a full line. The vessel boundary is the outer thick line.

saturated flattening of the T_e profile due to the “thermal shortcircuit” across the island develops when it locks with the O point in correspondence with the ECE radiometer. The radial profile of the temperature oscillations, or equivalently the displacement of flux surfaces outside the island, can be well reproduced assuming a magnetic perturbation proportional to the linear tearing mode eigenfunction $\tilde{\psi}_m$ [3]. The island width W is then obtained from the perturbation amplitude that fits the measured oscillation profile. The oscillation frequency transiently increases as ECRH is applied, then it slows down to locking, as shown in Fig. 4 for a pure $m = 2$, $n = 1$ mode (# 15469). In another case (# 14979) an $m = 1$ mode is excited as an $m - 1$ sideband by toroidal coupling to the $m = 2$, $n = 1$ tearing mode. The frequency evolution in this case (Fig. 5) is more complex than that of shot # 15469 because here, as explained below, there is a joint evolution of the $m = 1$ and $m = 2$ modes terminating with uncoupling of the $m = 1$ from the $m = 2$, while the latter locks to the wall.

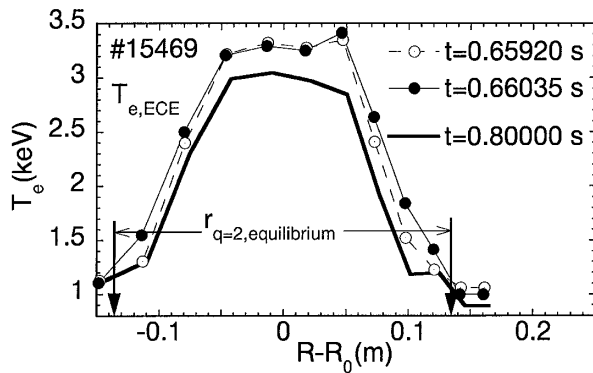


FIG. 3. Electron temperature profiles from fast ECE diagnostic (shot # 15469). Dotted line: Pulsating profile during rotation. Thick line: After oscillations have disappeared.

An interpretation of the observations and of the possible triggers of the modes can be given through a nonlinear dynamic model for the evolution of the island width and rotation frequency. Contributions that depend on the thermal energy increase and on the interaction with the resistive wall [4] as well as on the toroidal coupling with sideband modes of poloidal numbers $m, m \pm 1$ are included in the model. The model has been developed [5,6] extending the procedure introduced by Rutherford for large R/a , and reduced magnetohydrodynamic (RMHD) ordering [3,5,7]. A system of nonlinear coupled equations for the mode amplitudes and (toroidal) rotation frequencies is obtained, using the quasineutrality condition $\nabla \cdot \mathbf{J} = 0$ and Faraday and Ampere’s laws suitably averaged over the island region [3]:

$$\frac{dW_m}{dt} = \frac{r_{sm}^2}{\tau_{R_m}} \left[\Delta'_m + C_{m,m\pm 1} \frac{W_{m\pm 1}^2}{W_m^2} \cos(\Delta\phi) - f_R(\omega_m) \right], \quad (1)$$

$$\frac{d\omega_m}{dt} = \frac{1}{I_\phi^{(m)}} \left[D_{m,m\pm 1} W_{m\pm 1}^2 W_m^2 \sin(\Delta\phi) - W_m^4 h_m^2 f_I(\omega_m) - \omega_m \frac{dI_\phi^{(m)}}{dt} \right] - \mu_{\perp m} \frac{r_{sm}}{W_m} (\omega_m - \omega_{*m}). \quad (2)$$

Here r_{sm} , W_m , ω_m , τ_{R_m} , are, respectively, the m th rational surface radius, the island width, the instantaneous rotation frequency, and the effective resistive diffusion time scale, $h_m = Br_{sm}q'/16Rq^2$ and $q = rB/RB_\theta$ is the safety factor, ω_{*m} is the electron diamagnetic angular frequency, and $\Delta\phi = \phi_{m\pm 1} - \phi_m$ is the instantaneous phase difference between toroidal sidebands ($m \pm 1$) and master mode (m). The nonlinear function $\Delta'_m(W, \omega_m)$ is appropriately defined for each mode m (see below). The effective toroidal moment of inertia of the amount of plasma associated with an island of separatrix width W_m , rotating in a plasma of small viscosity $\mu_{\perp m}$, is $I_\phi^{(m)} = \lambda^{(m)} n_e m_i r_m R_0^3 W_m$, where the factor $\lambda^{(m)}$ is geometric. The coupling coefficients

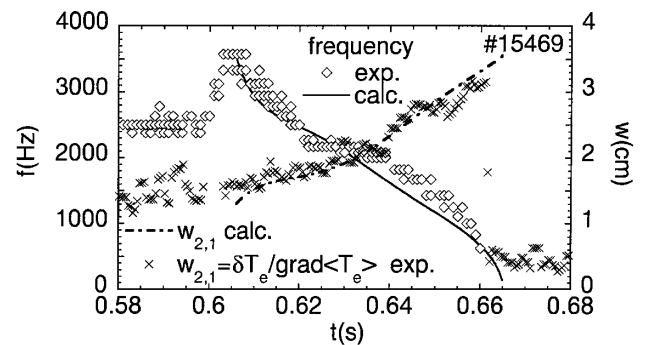


FIG. 4. Slowing down of the rotation frequency $\omega_{2,1}/2\pi$ and growth of the amplitude (W) of $m = 2$ mode in FTU shot # 15469. Full and dot-dashed lines were calculated by the theoretical model.

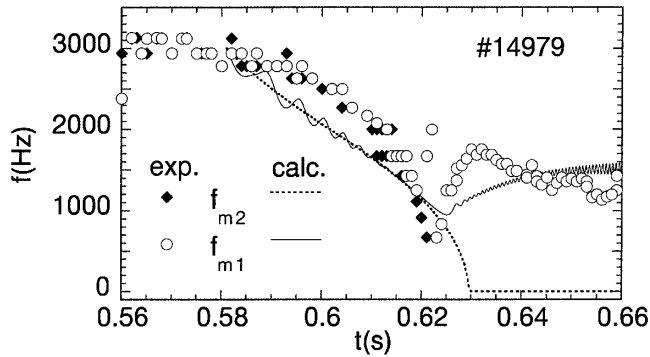


FIG. 5. Time evolution of the frequencies of the oscillations with $m = 1$ and $m = 2$ poloidal mode numbers in FTU shot # 14979 with $B = 5.6$ T. Diamonds correspond to $m = 2$ oscillations at $r \approx r_{q=2}$, open dots to $m = 1$ oscillations at $r \approx r_{q=1}$, and full and dashed lines are the result of the theoretical model.

$C_{m\pm 1,m}$ and $D_{m\pm 1,m}$ can be obtained, without loss of generality, from momentum balance conditions and an interaction model based on equivalent sheet currents [5,8]. The functions $f_R(\omega_m)$, $f_I(\omega_m)$ represent the real and imaginary part of the response of the wall (of radius d) to the time dependent magnetic perturbations:

$$f(\omega_m) = \frac{2m}{r_{sm}} \left(\frac{r_{sm}}{d} \right)^2 \frac{(\omega_m \tau_{wm})^2 + i \omega_m \tau_{wm}}{1 + (\omega_m \tau_{wm})^2} \quad (3)$$

for a circular large R/a geometry [4], where $\tau_{wm} \approx 2$ ms is the wall time constant. In a tokamak discharge normally operated at constant plasma current an intense ECRH localized near the $q \approx 1$ may steepen the gradient of the current density and increase the pressure near other rational q surfaces, namely the $q = 2$ surface, thus modifying the stability of $m = 2$ tearing modes. The tearing stability parameter given by $\Delta'_0 = \lim_{\epsilon \rightarrow 0} (d \ln B_r / dr)_{r_m^+}^{r_m^+ + \epsilon}$ is evaluated numerically outside the island with a RMHD tearing eigenfunction code using equilibrium q profiles obtained from resistive diffusion calculations. The sensitivity of the results to the accuracy of the q profile determination has been checked by varying the resistivity from Spitzer to neoclassical [this gives a 20% variation in $q(0)$]. The results with η_{Sp} for the FTU pulse # 15469 are $(r_2 \Delta'_0)_{Sp} \approx -0.66$ and $(r_2 \Delta'_0)_{neo} \approx -1.16$ at $t = 0.58$ s and $(r_2 \Delta'_0)_{Sp} \approx -0.98$ and $(r_2 \Delta'_0)_{neo} \approx -1.26$ at $t = 0.64$ s. In the general expression $\Delta'_m(W, \omega) = \Delta'_0(W) + \Delta'_{bs}(W) - \Delta'_{GGJ}(W) - \Delta'_{pol}(W, \omega)$ all the terms but the first one are proportional to $\beta_p = P/8\pi B_0^2$, where P is the plasma pressure, and describe the competition between the stabilizing polarization current $\Delta'_{pol}(W, \omega)$ [9], the term $\Delta'_{GGJ}(W)$ [10] and the bootstrap neoclassical effect $\Delta'_{bs}(W)$ [9–15]. The localized ECRH increases $\beta_p(r_{q=2})$ definitely above a critical value for which the destabilizing contribution, due to flattening of the bootstrap current across the initial “seed” island, dominates the other stabilizing effects [9–15]. The critical value is defined as

$\beta_{p,crit} \approx g(\epsilon, \nu_{ii}) \epsilon^{-3/4} \rho_{ip} (-\Delta'_{0,m}) (L_p/L_q)^{1/2}$; $L_{p,q}$ are the (slowly varying) pressure and safety factor scale lengths, ρ_{ip} the ion poloidal gyroradius, and $g(\epsilon, \nu_{ii}) \epsilon^{-3/4}$ a coefficient $O(1)$ related to the collisionality regime [9] with ν_{ii} the ion-ion collision frequency and $\epsilon = r/R$. After the turn on of the rf power, β_p increases clearly above the $\beta_{p,crit}$ (Fig. 6) and the island width increases as a consequence. As shown in Fig. 6 the temperature plateau size, related to the island size initially increases as β_p , but the island saturation is not yet reached when β_p levels off. The observed range of $\beta_p = 0.28$ – 0.4 and an initial $\beta_{p,crit} \approx 0.28$ estimated from the typical values of Δ'_0 is similar to that associated to the onset of neoclassical tearing modes in the COMPASS-D tokamak [13]. On the other hand, this behavior suggests that in FTU both current gradient and neoclassical effects contribute to the stability conditions of the $m = 2$, $n = 1$ mode. On the basis of the modeling through Eqs. (1) and (2), the following interpretation can be given of the evolution of the rotation frequency of the 2/1 mode in FTU shot # 15469 shown in Fig. 4. Before application of ECW power a marginally stable $m = 2$ mode is rotating at a constant frequency corresponding to the local electron diamagnetic frequency $\omega_{*m}/2\pi \approx 2.5$ kHz. The rf power input increases rapidly the pressure gradient and the diamagnetic frequency grows to ≈ 3.5 kHz while the mode appears significantly destabilized, starting its growth towards a large size rotating island. Subsequently ($t > 0.605$ s), the island slows down in two stages, identified by a change of concavity of the trace of the frequency vs time, with the inflection point at $t \approx 0.63$. The positive concavity of the first stage corresponds to the *inertial* slowing down effects due a growing moment of inertia ($\propto W$). The second stage ($t > 0.63$) of the frequency evolution, with negative concavity, corresponds to the well-known [4] braking torque $\propto W_m^4$ due to eddy currents, eventually leading to mode locking. This shows for the *first time* an inertial effect on the rotation of a magnetic island. The viscous drag $(\mu_{\perp} r_{sm}/W_m)(\omega - \omega_{*m})$, decreases as $1/W_m$ and is negligible in the incipient stage of deviation from the

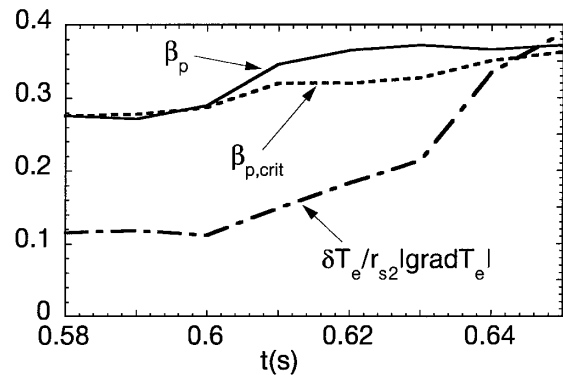


FIG. 6. Evolution of β_p , $\beta_{p,crit}$ and $\delta T_e / r_{s2} |\nabla T_e|$ for shot # 15469.

natural frequency ω_{*m} . This interpretation is supported by the results of the simulation shown in Fig. 4.

The second important case is shown in Fig. 5 (shot # 14979) together with the results of the complete theoretical model of coupled modes evolution. These equations describe the role and competition of the island inertia with the resistive wall braking torque and electrodynamic coupling with the sidebands. Coupling can have a stabilizing or destabilizing effect depending on the phase difference which evolves nonlinearly in a pendulumlike fashion. The stable fixed point of the coupled system in the $(\Delta\omega, \Delta\phi)$ phase space corresponds to a phase difference for which coupling has the largest destabilizing contribution [5]. During the ECRH pulse (Fig. 5) the $(m = 1, n = 1)$ and the $(m = 2, n = 1)$ modes initially rotate tightly coupled with a common frequency $\omega(t) \approx \omega_*(r_{q=2})$ controlled by

the larger $(2,1)$ island that is being slowed down by the resistive wall. Uncoupling of the modes occurs at $t = 0.62$, when $\omega(t)$ has reached the value close to the $(1,1)$ drift frequency [$\omega(t) \approx \omega_*(r_{q=1}) = \omega_{*1}$]. Since the coupling torque depends on the phase difference $\Delta\phi$ between the two modes, it is the severe wall braking of the $(2,1)$ that causes the uncoupling as the mutual torque becomes very ineffective for $\Delta\phi$ very different from zero. The $(1,1)$ internal mode of smaller amplitude and far away from the wall will keep rotating close to its *natural frequency* ω_{*1} dictated by the viscous torque, and eventually decreases in amplitude. The uncoupled $m = 2, n = 1$ island, closer to the wall, is eventually locked by the interaction with the wall eddy currents. The condition for unlocking of the coupled islands is a new important result of the equation governing the evolution of the phase difference between them:

$$\begin{aligned} \frac{d^2\Delta\phi}{dt^2} + aW_1^2W_2^2 \sin(\Delta\phi) = & d_1W_1^4f_I(\omega_1) + d_2W_2^4f_I(\omega_2) + \omega_1 \frac{d \ln W_1}{dt} \\ & - \omega_2 \frac{d \ln W_2}{dt} - \mu_{\perp 1} \frac{r_{s1}}{W_1} (\omega_1 - \omega_{*1}) + \mu_{\perp 2} \frac{r_{s2}}{W_2} (\omega_2 - \omega_{*2}), \end{aligned} \quad (4)$$

where a, d_1 , and d_2 are constant coefficients. The condition for unlocking is reached when the common frequency $\omega(t)$ is $\approx \omega_{*1}$ and the term related to the wall braking of the $(2,1)$ mode competes with the mutual torque $d_2f_I(\omega_2) \approx aW_1^2W_2^{-2}$, as has been verified numerically. In Figs. 4 and 5 the numerical results of the model show that the essential features of the experimental observations can be identified. This confirms the role of inertia and wall interaction in determining the phase relations necessary for coupling. In conclusion, we have provided a new experimental evidence and theoretical interpretation of paradigmatic cases, with relevant new physics clarifying the mechanisms of magnetic island rotation and coupling conditions in a regime of tearing modes driven by an increase of the electron thermal energy and J profile reshaping.

-
- [3] P.H. Rutherford, *Phys. Fluids* **6**, 1903 (1973).
 [4] M.F. Nave and J.A. Wesson, *Nucl. Fusion* **30**, 2575 (1990).
 [5] R. Coelho and E. Lazzaro, in *Theory of Fusion Plasmas: Proceedings of the Joint Varenna-Lausanne International Workshop, Varenna, Italy, 1998* (ISPP-18), edited by J.W. Connor, E. Sindoni, and J. Vaclavik (Società Italiana di Fisica, Bologna, 1999), p. 395.
 [6] M.F.F. Nave, R. Coelho, E. Lazzaro, and F. Serra, *Eur. Phys. J. D* **8**, 287 (2000).
 [7] M.N. Rosenbluth, D.A. Monticello, H. Strauss, and R.B. White, *Phys. Fluids* **19**, 1987 (1977).
 [8] R. Coelho, E. Lazzaro, M.F.F. Nave, and F. Serra, *Phys. Plasmas* **6**, 1194 (1999).
 [9] A.I. Smolyakov *et al.*, *Phys. Plasmas* **2**, 1581 (1995).
 [10] A. Glasser, J.M. Greene, and J.L. Johnson, *Phys. Fluids* **18**, 875 (1975).
 [11] C.C. Hegna and J.D. Callen, *Phys. Fluids B* **4**, 1855 (1992).
 [12] R. Fitzpatrick, *Phys. Plasmas* **2**, 825 (1995).
 [13] D.A. Gates *et al.*, *Nucl. Fusion* **37**, 1593 (1997).
 [14] Z. Chang *et al.*, *Phys. Rev. Lett.* **74**, 4663 (1995).
 [15] O. Sauter *et al.*, *Phys. Plasmas* **4**, 1654 (1997).

-
- [1] S. Cirant *et al.*, in *Radio Frequency Power in Plasmas*, AIP Conf. Proc. No. 485 (AIP, New York, 1999), p. 221.
 [2] G. Ramponi *et al.*, in *Radio Frequency Power in Plasmas* (Ref. [1]), p. 265.